Nanometer-scale optical imaging of collagen fibers using gold nanoparticles

Bo Chen,[1] Laura C. Estrada,[1] Christian Hellriegel,[1,2] and Enrico Gratton[1,*]

[1]Laboratory for Fluorescence Dynamics, Biomedical Engineering Department, University of California, Irvine, USA.
[2]*Microscopy and Dynamic Imaging Unit, CNIC (Centro Nacional de Investigaciones Cardiovasculares), Madrid, Spain.*
egratton@uci.edu

Abstract: We describe 3D single particle tracking of gold nanoparticles (AuNPs) moving along collagen fibers in aqueous environment with two-photon excitation conditions. The photoacoustic effect at the collagen fiber caused by the irradiation with ultrashort, near-infrared laser pulses propels the particles adsorbed to the surface of the collagen fibers. We report the tracking of individual AuNPs in three dimensions with high spatial and temporal resolution, of few nanometers and milliseconds, respectively. Due to the emission signal caused by the interaction between the AuNPs and the weak chromophores in the collagen fiber, the trajectories of individual AuNPs reveal the fiber topography with nanometric resolution. The intensity along the trajectory shows that we are sensitive to the distribution of the weak chromophores on the fiber.

OCIS codes: (170.0180) Microscopy; (300.6280) Spectroscopy, fluorescence and luminescence; (110.5125) Photoacoustics; (160.4236) Nanomaterials.

References and links

1. B. M. Kim, J. Eichler, K. M. Reiser, A. M. Rubenchik, and L. B. Da Silva, "Collagen structure and nonlinear susceptibility: effects of heat, glycation, and enzymatic cleavage on second harmonic signal intensity," Lasers Surg. Med. **27**(4), 329–335 (2000).
2. P. Odetti, M. A. Pronzato, G. Noberasco, L. Cosso, N. Traverso, D. Cottalasso, and U. M. Marinari, "Relationships between glycation and oxidation related fluorescences in rat collagen during aging. An in vivo and in vitro study," Lab. Invest. **70**(1), 61–67 (1994).
3. S. Tanaka, G. Avigad, B. Brodsky, and E. F. Eikenberry, "Glycation induces expansion of the molecular packing of collagen," J. Mol. Biol. **203**(2), 495–505 (1988).
4. G. Falzon, S. Pearson, R. Murison, C. Hall, K. Siu, A. Evans, K. Rogers, and R. Lewis, "Wavelet-based feature extraction applied to small-angle x-ray scattering patterns from breast tissue: a tool for differentiating between tissue types," Phys. Med. Biol. **51**(10), 2465–2477 (2006).
5. M. Okuda, M. Takeguchi, M. Tagaya, T. Tonegawa, A. Hashimoto, N. Hanagata, and T. Ikoma, "Elemental distribution analysis of type I collagen fibrils in tilapia fish scale with energy-filtered transmission electron microscope," Micron **40**(5-6), 665–668 (2009).
6. L. Bozec, G. van der Heijden, and M. Horton, "Collagen fibrils: nanoscale ropes," Biophys. J. **92**(1), 70–75 (2007).
7. P. J. Campagnola, A. C. Millard, M. Terasaki, P. E. Hoppe, C. J. Malone, and W. A. Mohler, "Three-dimensional high-resolution second-harmonic generation imaging of endogenous structural proteins in biological tissues," Biophys. J. **82**(1), 493–508 (2002).
8. E. Rittweger, K. Y. Han, S. E. Irvine, C. Eggeling, and S. W. Hell, "STED microscopy reveals crystal colour centres with nanometric resolution," Nat. Photonics **3**(3), 144–147 (2009).
9. A. Yildiz, J. N. Forkey, S. A. McKinney, T. Ha, Y. E. Goldman, and P. R. Selvin, "Myosin V walks hand-over-hand: single fluorophore imaging with 1.5-nm localization," Science **300**(5628), 2061–2065 (2003).
10. C. Sönnichsen, S. Geier, N. E. Hecker, G. von Plessen, J. Feldmann, H. Ditlbacher, B. Lamprecht, J. R. Krenn, F. R. Aussenegg, V. Z.-H. Chan, J. P. Spatz, and M. Möller, "Spectroscopy of single metallic nanoparticles using total internal reflection microscopy," Appl. Phys. Lett. **77**(19), 2949–2951 (2000).
11. R. Yasuda, H. Noji, M. Yoshida, K. Kinosita, Jr., and H. Itoh, "Resolution of distinct rotational substeps by submillisecond kinetic analysis of F1-ATPase," Nature **410**(6831), 898–904 (2001).
12. K. Ritchie, X.-Y. Shan, J. Kondo, K. Iwasawa, T. Fujiwara, and A. Kusumi, "Detection of non-Brownian diffusion in the cell membrane in single molecule tracking," Biophys. J. **88**(3), 2266–2277 (2005).
13. X. L. Nan, P. A. Sims, and X. S. Xie, "Organelle tracking in a living cell with microsecond time resolution and nanometer spatial precision," ChemPhysChem **9**(5), 707–712 (2008).

#137496 - $15.00 USD Received 1 Nov 2010; revised 14 Jan 2011; accepted 4 Feb 2011; published 7 Feb 2011

14. J. Gelles, B. J. Schnapp, and M. P. Sheetz, "Tracking kinesin-driven movements with nanometre-scale precision," Nature **331**(6155), 450–453 (1988).
15. G. Louit, T. Asahi, G. Tanaka, T. Uwada, and H. Masuhara, "Spectral and 3-dimensional tracking of single gold nanoparticles in living cells studied by Rayleigh light scattering microscopy," J. Phys. Chem. C **113**(27), 11766–11772 (2009).
16. K. Lindfors, T. Kalkbrenner, P. Stoller, and V. Sandoghdar, "Detection and spectroscopy of gold nanoparticles using supercontinuum white light confocal microscopy," Phys. Rev. Lett. **93**(3), 037401 (2004).
17. L. Cognet, C. Tardin, D. Boyer, D. Choquet, P. Tamarat, and B. Lounis, "Single metallic nanoparticle imaging for protein detection in cells," Proc. Natl. Acad. Sci. U.S.A. **100**(20), 11350–11355 (2003).
18. O. Thoumine, H. Ewers, M. Heine, L. Groc, R. Frischknecht, G. Giannone, C. Poujol, P. Legros, B. Lounis, L. Cognet, and D. Choquet, "Probing the dynamics of protein-protein interactions at neuronal contacts by optical imaging," Chem. Rev. **108**(5), 1565–1587 (2008).
19. M. A. van Dijk, M. Lippitz, D. Stolwijk, and M. Orrit, "A common-path interferometer for time-resolved and shot-noise-limited detection of single nanoparticles," Opt. Express **15**(5), 2273–2287 (2007), http://www.opticsinfobase.org/oe/abstract.cfm?URI=oe-15-5-2273.
20. E. Katz and I. Willner, "Integrated nanoparticle-biomolecule hybrid systems: synthesis, properties, and applications," Angew. Chem. Int. Ed. Engl. **43**(45), 6042–6108 (2004).
21. J. Sharma, R. Chhabra, A. Cheng, J. Brownell, Y. Liu, and H. Yan, "Control of self-assembly of DNA tubules through integration of gold nanoparticles," Science **323**(5910), 112–116 (2009).
22. Y. Arntz, L. Jourdainne, G. Greiner-Wacker, S. Rinckenbach, J. Ogier, J. C. Voegel, P. Lavalle, and D. Vautier, "Immunogold detection of types I and II chondrocyte collagen fibrils: an in situ atomic force microscopic investigation," Microsc. Res. Tech. **69**(4), 283–290 (2006).
23. D. E. Birk, J. M. Fitch, J. P. Babiarz, and T. F. Linsenmayer, "Collagen type I and type V are present in the same fibril in the avian corneal stroma," J. Cell Biol. **106**(3), 999–1008 (1988).
24. X. Mo, Y. J. An, C. S. Yun, and S. M. Yu, "Nanoparticle-assisted visualization of binding interactions between collagen mimetic peptide and collagen fibers," Angew. Chem. Int. Ed. Engl. **45**(14), 2267–2270 (2006).
25. P. Friedl, K. Wolf, U. H. von Andrian, and G. Harms, "Biological second and third harmonic generation microscopy", in *Current Protocols in Cell Biology*, J. S. Bonifacino, M. Dasso, J. B. Harford, J. Lippincott-Schwartz, and K. M. Yamada, eds. (Wiley, 2007), Chap. 4.
26. Y. C. Guo, H. E. Savage, F. Liu, S. P. Schantz, P. P. Ho, and R. R. Alfano, "Subsurface tumor progression investigated by noninvasive optical second harmonic tomography," Proc. Natl. Acad. Sci. U.S.A. **96**(19), 10854–10856 (1999).
27. C. Hellriegel and E. Gratton, "Real-time multi-parameter spectroscopy and localization in three-dimensional single-particle tracking," J. R. Soc. Interface **6**(0 Suppl 1), S3–S14 (2009).
28. R. A. Kruger, and P. Liu, "Photoacoustic ultrasound: pulse production and detection of 0.5% Liposyn," Med. Phys. **21**(7), 1179–1184 (1994).
29. R. A. Kruger P. Y. Liu, Y. R. Fang, and C. R. Appledorn, "Photoacoustic ultrasound (PAUS)--reconstruction tomography," Med. Phys. **22**(10), 1605–1609 (1995).
30. J. A. Viator, L. O. Svaasand, G. Aguilar, B. Choi, and J. S. Nelson, "Photoacoustic measurement of epidermal melanin," Proc. SPIE **4960**, 14–20 (2003).
31. T. P. Taube, M. B. Puzzi, J. Rehder, A. M. Mansanares, E. C. da Silva, D. Acosta-Avalos, and P. R. Barja, "Characterization of reconstructed human skin using photoacoustic spectroscopy," Eur. Phys. J. Spec. Top. **153**(1), 471–474 (2008).
32. S. Mallidi, T. Larson, J. Aaron, K. Sokolov, and S. Emelianov, "Molecular specific optoacoustic imaging with plasmonic nanoparticles," Opt. Express **15**(11), 6583–6588 (2007).
33. S. Mallidi, T. Larson, J. Tam, P. P. Joshi, A. Karpiouk, K. Sokolov, and S. Emelianov, "Multiwavelength photoacoustic imaging and plasmon resonance coupling of gold nanoparticles for selective detection of cancer," Nano Lett. **9**(8), 2825–2831 (2009).
34. L. Wang, *Photoacoustic Imaging and Spectroscopy* (CRC Press, (2009), p. 483
35. V. Levi, Q. Q. Ruan, and E. Gratton, "3-D particle tracking in a two-photon microscope: application to the study of molecular dynamics in cells," Biophys. J. **88**(4), 2919–2928 (2005).
36. K. Kis-Petikova and E. Gratton, "Distance measurement by circular scanning of the excitation beam in the two-photon microscope," Microsc. Res. Tech. **63**(1), 34–49 (2004).

1. Introduction

Collagen forms the structural network of the extracellular matrix in tissue and is the most abundant protein in vertebrates. At the molecular level, type I collagen consists of three left-handed polypeptide strands twisted together into a rod-shaped, triple-helix tertiary conformation stabilized by numerous hydrogen bonds. Fibers are formed by bundles of the triple-helix basic element. Understanding both the structural and functional properties of fibrillar collagen type I is of considerable interest to many researchers, particularly those in the medical field because the structural modifications of the fibrillar matrix are associated with various physiologic processes such as diabetes, aging, wound healing, and cancer [1–3]. Changes in the collagen nanostructure have been used to identify breast tissue malignancy [4].

#137496 - $15.00 USD Received 1 Nov 2010; revised 14 Jan 2011; accepted 4 Feb 2011; published 7 Feb 2011

Several methods such as electron microscopy [5], atomic force microscopy (AFM) [6] and second-harmonic generation microscopy [7] have been used to characterize the structure of collagen. Although the first two methods have very high spatial resolution, the samples need to be fixed and/or dried so it is hard to obtain dynamic structural information. On the other hand, methods based on far field optical microscopy do not require fixation, but the spatial resolution is diffraction limited unless super-resolution techniques are used [8].

In this paper we describe an optical method used to explore the dynamic spatial structure of collagen type I rat tail fibers. We use a probe that we can move along the fiber and which we can track in three-dimensional space with nanometer accuracy. The optical principle is similar in concept to methods like FIONA (Fluorescence Imaging with One Nanometer Accuracy) that have been successfully used to track the movement of motor proteins along microtubules or along actin fibers [9] with nanometer accuracy in two dimensions. The ideal probe for the application of this technology must fulfill two apparent contradictory prerequisites: It should generate an intense optical signal, but at the same time be as small as possible, so as to explore features on the surface of the object with high fidelity. Gold nanoparticles (AuNPs) are very appealing for this purpose because they do not photobleach or blink and do not optically saturate at reasonable exciting intensities. Because of the relatively high scattering cross section, large AuNPs ($R \sim \lambda$, where R is the particle radius and λ the excitation wavelength) can be imaged using optical methods such as total internal reflection [10], video-based contrast enhancement [11,12], asymmetric dark-field illumination [13] and imaging scattered light [14,15]. However, it is still a challenge to detect small particles ($R << \lambda$) since their scattering signal scales with the sixth power of the particle diameter [16]. To address this problem, new techniques such as photo-thermal interference contrast [17,18] and interferometric detection [19] have been developed to increase the signal-to-noise ratio and thus allow for the detection of small sizes AuNPs with high sensitivity. Nevertheless, AuNPs have become popular as immuno-labeling markers for visualization tools [20–22]. Antibody-passivated and peptide-assisted AuNPs were successfully used to identify specific types of collagen fibers in tissue and visualization of binding between collagen mimetic peptide and collagen fibers, respectively [23,24]. However, in the previous references, the gold particles are immobilized and they are not used to trace the topography of the underlying substrate.

Two-photon excitation (TPE) microscopy has developed into a popular and powerful approach due to three well-known advantages: (*i*) reduced photo toxicity of the near-infrared excitation; (*ii*) lack of off-focus excitation; (*iii*) a wide excitation range of many fluorophores compared to single photon excitation, allowing multicolor imaging using the same excitation wavelength [25]. Guo et al. [26] originally used second-harmonic generation (SHG) microscopy to image within muscle and tissue, where frame rates of several hours were required. Later, Mohler et al. [7] extended this imaging concept to higher resolution (~1 μm) and higher rates of image acquisition (1 frame/s).

Here, we present a scheme to obtain the local structure of collagen fibers by tracking the movement of AuNPs moving along the fibers. To follow the movement of the particle we use the 3D orbital tracking method with high-resolution (2-20 nm) which employs TPE excitation [27]. We also describe the physical mechanism that allows AuNPs to perform a directed motion along collagen fibers.

2. Material and Methods

Chemicals: 5, 20, and 40 nm diameter AuNPs were commercially available (Ted Pella, USA). Cell culture media were from Sigma and Invitrogen (USA) and acid soluble rat tail tendon collagen type I from BD Biosciences (USA).

Sample hydrogel preparation: All materials were placed on ice for half an hour for the preparation of the collagen hydrogels: acid soluble rat tail tendon collagen type I (BD Biosciences, San Jose, CA, USA) and DMEM High Glucose (4.5 g/L, without L glutamine, with sodium Pyruvate 110 mg/L, phenol red free). Two reagents, 5X Dulbecco's Modified Eagle's Medium (DMEM) (Sigma, St. Louis, MO) and 10X reconstitution buffer were also needed and prepared respectively by combining one bottle of phenol red-free DMEM powder

#137496 - $15.00 USD Received 1 Nov 2010; revised 14 Jan 2011; accepted 4 Feb 2011; published 7 Feb 2011

(Sigma-Aldrich, USA) with 200 ml double deionized water (ddH_2O) pH balanced to 7.9-8.0 by the addition of 1M sodium hydroxide (NaOH) and mixing 2.2 g sodium bicarbonate, 4.8 g HEPES with 100 ml ddH_2O. Both reagents were filter sterilized. For each gel, 30 µl of the 10X reconstitution buffer, 60 µl of 5X DMEM, 64 µl of collagen type I high-concentration (9.44 mg/ml) and 146 µl of DMEM-High Glucose was combined in that order and vortexed for 3-4 seconds. The final mixture with concentration 2 mg/ml and volume 300 µl was immediately pipetted into a 35 mm imaging dish, No.1.5 coverglass (Mat Tek Corporation, MA, USA) and incubated at room temperature for one hour. The AuNPs of 5, 20 and 40 nm in diameter are available as suspensions (BBinternational, UK) and were sonicated prior to use. 30 µl of the gold suspension were added into the gel. Figure 1 shows a Transmission Electron Microscopy of a sample were NP's concentration was dramatically increased relative to a typical sample for imaging purposes.

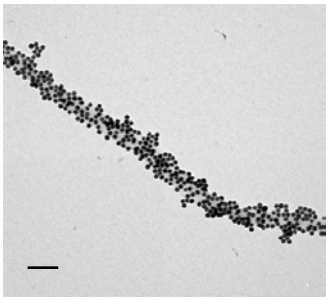

Fig. 1. TEM image of a collagen fiber coated with 20 nm AuNPs. Scale bar: 100 nm

Transmission electron microscopy (TEM) sample preparation: Collagen fibril suspensions were adsorbed to the Formvar-coated grids for 30 s, washed with ddH_2O several times, negatively stained with uranyl acetate to enhance contrast and air-dried at room temperature. TEM images were obtained on a FEI/Philips CM20 electron microscope operated at 80kV.

Microscopy set-up for multi-parameter acquisition: The two-photon microscope system used in this work has been described previously [27]. Briefly, the excitation light was provided by a mode-locked 80 MHz Ti:Sapphire laser (Chameleon Ultra, Coherent Inc., Palo Alto, CA, USA) with integrated Verdi tunable from 690 to 1040 nm. We used an UPlanFL N 60X 0.9 NA air objective (Olympus, Japan) and a shortpass dichroic mirror (700DCSPXR, Chroma Technologies, VT, USA) to direct the excitation light into the sample. Additionally a HQ700LP filter (Chroma) was positioned before the dichroic to filter out the Ti:Sapphire fluorescence. The average laser irradiation after the microscope objective was measured with an Ultracompact Laser Power Meter (New Focus Corp., CA, USA), which ranged from 0.5 to 2 mW. Fluorescence and SHG signals from the fibers were detected through an emission filter (ET680SP, Chroma Technologies, VT, USA) and split into two channels using a dichroic mirror (485DCLP, Chroma). In the first channel, the SHG images were detected through a bandpass filter (HQ435/70, Chroma). In the second channel, the fluorescence was detected through a bandpass filter (HQ610/75, Chroma). Both signals were detected with photomultiplier tubes (H7422P-40, Hamamatsu, Japan). Finally, signal was amplified (ACA-4-35N, Becker&Hickl, Germany), discriminated (Model 6915, Phillips Scientific, NJ, USA), and TTL pulses were counted by the ISS 3-axis data acquisition card (ISS, IL, USA). Alternatively, the emission from the sample can be analyzed with a custom-made prism-CCD spectrometer (CCD from Princeton Instruments, NJ, USA). Three dimensional scanning was obtained using galvano motor-driven scanning mirrors (6350, Cambridge Technology Inc., MA, USA) with controller series 603X servo system (60335 FM, Cambridge Technology Inc., MA, USA), and a PIFOC P-721 piezo-driven objective device (Physics Inst., Germany). Both galvano and piezo were driven by an ISS 3-axis card (ISS, IL, USA). Experiments were controlled by a commercially available data acquisition program (SimFCS, IL, USA).

#137496 - $15.00 USD Received 1 Nov 2010; revised 14 Jan 2011; accepted 4 Feb 2011; published 7 Feb 2011

Orbital Tracking: The principle of orbital tracking has been discussed in detail in previous references [27,35,36]. Briefly, during a standard cycle of the orbital tracking method, the laser beam traces n circular orbits around the particle to track in two z planes, one above and one below the particle. The radius of the orbits is equal to half the radial waist of the microscope point spread function (PSF), whereas the distance between the two planes is equal to the axial waist of the PSF. When the particle is at the center of the orbit, the fluorescence intensity is constant as the laser beam performs the orbit. However, when the particle moves from the center of orbit, this leads to a modulation of the fluorescence signal. The main purpose of the feedback algorithm for orbital particle tracking is finding the particle position after it has moved off the centre, and then rapidly (in few milliseconds) re-centering the particle at the new position. The automatic feedback is realized by using an algorithm based on the fast Fourier transformation of the intensity along the orbit using the first two Fourier coefficients. The modulation, defined as the quotient MOD = AC/DC (the first two Fourier coefficients), serves as an indicator for the distance from the particle to the orbit center. The z-position of the particle can be determined by performing an orbit slightly above and one slightly below the center of the particle. The z-focus will then move in the direction that minimizes the difference between the up and down orbit. This achieves three-dimensional tracking of the position of the particle. The accuracy of the position of the particle is determined by the linearity of the x-y and z position detectors, while the precision of the position is solely determined by the number of photons that can be collected during an orbit. Since the correction of the center position of the orbit is applied every 4 ms, but the intensity along the orbit is continuously measured, the actual position of the particle can be obtained at each orbit, irrespective of the period of the correction. Therefore, we can calculate the position with a resolution of the orbital period which is 1 ms in our setup. It is important to discuss in this paper, that the laser beam continuously tracks the position of the AuNP so that the spectrum of the emission from the particle can be continuously measured, even if the particle is rapidly moving.

2. Results

2.1. AuNPs movement along collagen fibers

Figure 2 shows the trails produced by nm-size AuNPs (5, 20 and 40 nm) embedded on a collagen fiber matrix during a single acquisition frame when using a raster scanning two-photon microscope. The white dots are stationary AuNPs while the collagen fibers are visualized via the second-harmonic generation signal (SHG) occurring at the fibers (in purple). The white spots were fit with a Gaussian function obtaining a half width which agrees with the value expected according to the microscope resolution. Figure 2 also shows that the AuNPs trails occur along a collagen fiber while the NPs which are far from a fiber remains almost stationary.

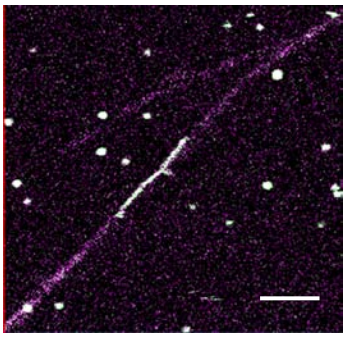

Fig. 2. Color overlay of the SHG signal produced at the collagen fibers (in purple) and the two-photon signal (in white) from 40 nm AuNPs when excited at 790 nm. Scale bar: 2 μm.

#137496 - $15.00 USD Received 1 Nov 2010; revised 14 Jan 2011; accepted 4 Feb 2011; published 7 Feb 2011

2.2. Characterization of the signal from AuNPs embedded on collagen fibers

Figure 2 shows both the SHG produced at the collagen fibers and the signal from the AuNPs, when excites at 790 nm. In order to characterize these processes we performed a two-photon excitation test and a single point spectral characterization. We measured the excitation power dependence of the emitted signal from a AuNP. The slope in a log-log plot resulted to be 2.0±0.1. This is expected for a second-order mechanism. Then, using a custom built spectrometer described previously [27] we park the excitation beam at a specific point of the sample that contains both a 5 nm AuNP and a visible collagen fiber (note that due to spatial alignment and phase-matching criteria, not all collagen fibers produce SHG) and retrieve the combined spectrum. Changing the wavelength of the laser from 960 to 840 nm (but maintaining the average power), we can observe the shift of the narrow SHG peak from 480 to 420 nm (indicated by arrows) in the spectrum, Fig. 3. However, the red-shifted and comparatively broad spectrum of the AuNP remained constant (note that also the fine structure of the spectrum remains constant while changing the excitation wavelength). The gray region in the figure indicates the filter cutoff wavelength.

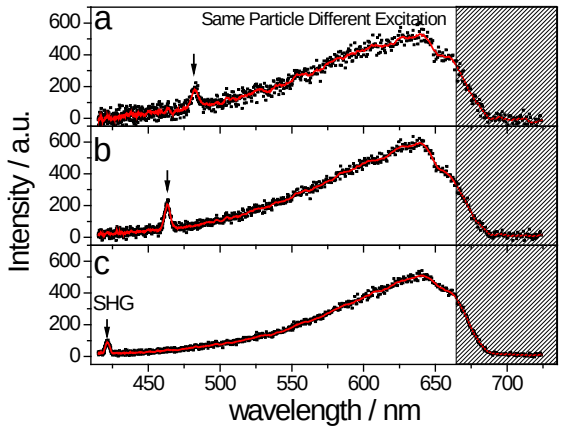

Fig. 3. Typical SHG and TPE combined spectra from AuNPs embedded on collagen fibers under different excitation wavelengths but the same power. (a) λexc = 960nm, (b) λexc = 920nm, (c) λexc = 840nm. The gray region indicates the filter cutoff wavelength.

2.3. 3D mapping of the fluorescence of collagen fibers using AuNPs

We used the fluorescent signal from label-free collagen fibers interacting with a single AuNP to map the collagen structure. Due to low range of the interaction process (1-10 nm), the NP's 3D trajectory reflects the underlying structure of collagen with nanometer resolution. Figure 4a shows a typical 3D particle trajectory of a 5 nm AuNP when moving on collagen. Each point in the Figure represents one position of the NP during the experiment, while the colors changes with intensity. The color scale ranges from 10 counts (in dark blue) to 150 counts (in dark red) meaning that the local interaction with the fiber determines the level of emission, i.e., there are "hot spots" along the fiber. The position of the "hot spots" is highly reproducible when scanning back and forth the same fiber. This observation is incompatible with a constant emission from the gold and suggests that the emission is modulated by the collagen chromophores, meaning that we are sensitive to the chromophores on the fiber.

However, using the same excitation power as in Fig. 4a, Fig. 4b shows the 3D trajectory of a NP which is confined to a short segment of 100 nm in length and approximately 30 nm across of a collagen fiber. In this case, because the particle explores this particular segment for a longer time, the 3D trajectory delineates the collagen fiber showing in more detail the

#137496 - $15.00 USD Received 1 Nov 2010; revised 14 Jan 2011; accepted 4 Feb 2011; published 7 Feb 2011

appearance of regions separated by few 10s of nanometers that affect the luminescence of the NP.

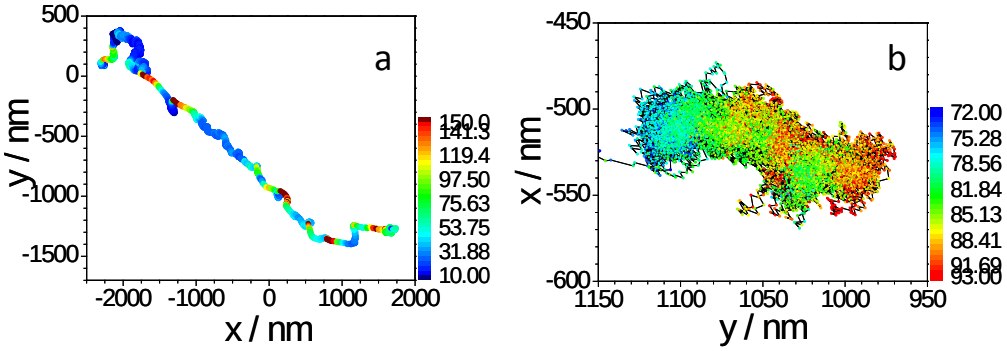

Fig. 4. 3D particle trajectory of a 5 nm AuNP when moving on a collagen fiber (a), and when it remains stationary (b). Note the different scales.

3. Discussion

3.1. AuNP's movement characterization

During the raster scanning imaging using TPE of nm-size AuNPs (5, 20 and 40 nm) embedded on a collagen fibers matrix, we found that some of the NPs move along the fibers in a single frame. The motion occurs in different directions and with different velocities, but not randomly. As an example, the bright dots in the Movie S1 (Supplemental material) are the diffraction limited patterns produced by 40 nm AuNPs. A single frame from this movie is shown in Fig. 2. In the absence of collagen fibers, when a suspension of AuNPs is deposited on a glass surface, we find that the majority of AuNPs remain stationary, or move very slowly in a random motion. Similarly, the AuNPs also remain stationary when excited using low power CW lasers, as used for one-photon excitation experiments. This behavior does not change in the presence of collagen fibers. The motion of AuNPs on the fibers were only observed when images were acquired using the ultrashort pulses of the Ti:Sapphire laser, typically used for TPE microscopy. The origin of the AuNPs movement seems to be linked to the excitation light. To investigate this, we first changed the excitation average power and the laser scanning direction. In a different experiment we studied the NPs movements as a function of the distance between two successive lines in the raster scan.

The occurrence of the AuNP motion gradually reduced until ultimately vanished as the excitation average power was decreased below 0.5 mW measured at the sample position. We also observed that the AuNPs moved faster in the same direction of the scan pattern (the scan pattern is from top to bottom and from left to right of the image) than in the reverse direction (from bottom to top and/or from right to left). Then we studied the NPs movements as a function of scanning parameters such as the distance between two successive lines in the raster scan, Δd. We observed that as Δd increased, the AuNPs fast movement almost vanished. Based on these observations, we propose that the appearance of trails in a single image occurs because the laser beam "kicks" the AuNPs forward during each line of the raster scan (we will explain, in the next section, the physical origin of this "kick"). The AuNP moves forwards along the collagen fiber for a short length at each line pass. Because the AuNPs are spherically symmetric, directed movement can only occur due to a force that is systematically applied in the same average direction. It appears that AuNPs are confined to be on a fiber, which makes them move only along the fiber itself. The AuNP movement along the fibers depends on the distance between two successive lines in the raster scan, the excitation wavelength, the average laser power and the position of the particle with respect to the scan line. This scenario is diagramed in Fig. 5.

#137496 - $15.00 USD Received 1 Nov 2010; revised 14 Jan 2011; accepted 4 Feb 2011; published 7 Feb 2011

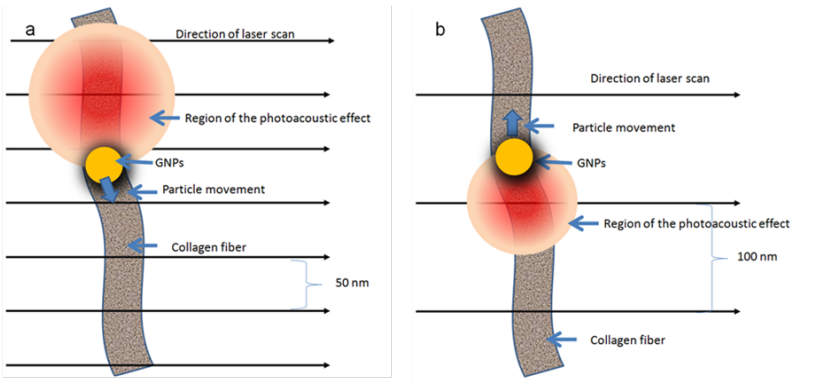

Fig. 5. Schematic representation of a AuNP moving along a collagen fiber under raster scanning mode. (a) the AuNP will move down when the laser beam passes at a position which is above the particle, (b) the AuNP will move up when the laser beam passes through a position which is below the particle.

According to our model, when the laser beam passes at a position which is above the particle, the particle will move forward in the direction of the raster scan, toward the bottom of the frame (Fig. 5a). When the laser beam passes through a position that is below the particle it will cause the particle to move up, against the raster scan direction, toward the top of the frame (Fig. 5b). When the particle moves down, there is a chance that the next line will produce again a motion toward the bottom of the frame if the separation of the lines is comparable to the size of the particle movement. This mechanism will repeat line after line and cause a cascade motion in which the particle moves along a fiber in a single frame—making the trajectory appear as a trail. Instead, for a particle that moves up, this motion does not repeat line after line, so the motion against the raster scan direction is not observed within the same frame but in consecutive frames—this motion does not produce trails.

3.2. Physical mechanism responsible for motion of AuNP along collagen fibers

It is well established that when tissues are irradiated with short-laser pulses, there is a rapid local thermo-elastic expansion due to the energy conversion from light to heat which induces a pressure wave propagating away from the point of energy deposition [28,29]. This process is known as the opto-acoustic or photoacoustic effect (PA). The PA effect has been found in tissues and in skin [30,31]. Collagen fibers are the major components of skin's dermis and spherical AuNPs have been used to detect cancer cells in vitro using PA methods [32,33]. Physical parameters such as expansion coefficient, specific heat, acoustic velocity, acoustic impedance, acoustic attenuation and thermal conductivity strongly affect PA generation and propagation. These parameters are functions of temperature. We studied the effects of AuNPs laser induced movement by changing the temperature of the sample. The phenomena of stepping the particle at each line of the frame can easily be seen at room temperature. However, we measured that when the sample temperature was lowered to 4°C, where the coefficient of thermal expansion of water is zero [34], the above phenomena disappeared. Based on the lack of motion at 4°C, we propose that the driving force of AuNPs stepping along a collagen fiber is due to PA effect which originates on the collagen fiber due to near-infrared absorption of the excitation light that couples to the surrounding solvent. The pressure wave generated by this effect is sufficient enough to move the AuNP by a certain step each time the laser hits the fibers near the location of the AuNP. Of course, the PA effect occurs independently on the presence of the AuNPs, but we can see its manifestation only when an AuNP is on the collagen fiber.

#137496 - $15.00 USD Received 1 Nov 2010; revised 14 Jan 2011; accepted 4 Feb 2011; published 7 Feb 2011

5. Conclusions

We investigated the movement of nm-size AuNPs along rat tail tendon collagen type I fibers. The work gives a detailed description of the experimental observations under two-photon excitation as well as a model to support the experiments. Our model, that describes accurately the measured data, propose that the driving force of AuNPs stepping along a collagen fiber is due to photoacoustic effect which originates on the collagen fiber due to near-infrared absorption of the excitation light that couples to the surrounding solvent. We provide experimental evidence of the capability to move gold NPs along collagen fibers. This opens the possibility of mapping fibers in 3D and with nanometer resolution using a two-photon microscope. Moreover, this opens the promising possibility of high-resolution studies of tissue and cells using NPs probes.

Acknowledgments

This work is supported in part by NIH P41 P41-RRO3155 and P50-GM076516. We would like to thank Gian-Guo Zheng and the Nanomaterials Characterization and Fabrication Facility (NCF2) for help us with TEM images. We also thank Kandice Tanner for help with the initial collagen samples preparation.

#137496 - $15.00 USD Received 1 Nov 2010; revised 14 Jan 2011; accepted 4 Feb 2011; published 7 Feb 2011